Ti-2007 Science and Technology, edited by M. Ninomi, S. Akiyama, M. Ikeda, M. Hagiwara, K. Maruyama
The Japan Institute of Metals (2007)

High Temperature Shape Memory Behavior in Ti-Ta Alloys

Pio John S. Buenconsejo[1], Hee Young Kim[1], Tamotsu Koyano[1], Hideki Hosoda[2], Shuichi Miyazaki[1]*

[1] *Institute of Materials Science, University of Tsukuba, Tsukuba 305-8573, Japan*
[2] *Precision and Intelligent Laboratory, Tokyo Institute of Technology, Yokohama 226-8503, Japan*
**Corresponding author, E-mail: miyazaki@ims.tsukuba.ac.jp*

Ti-Ni shape memory alloy (SMA) has transformation temperatures below 373K, setting the limitations of their applications. Therefore, SMAs with transformation temperatures above 373K have been developed, such as Ti-Ni-X (X=Zr, Hf, Au, Pd, Pt), but they exhibit poor cold-workability. The Ti-X (X=Nb, Ta, Mo) base alloys undergo martensitic transformation and have excellent cold-workability. However, Ti-Nb and Ti-Mo base alloys are very sensitive to aging because of the ω-phase formation. The ω-phase suppresses the transformation temperatures and causes embrittlement of the alloys. Previously our group has reported that the addition of Ta to Ti-Nb base alloys is effective to suppress the formation of ω-phase. In this study, we propose the development of Ti-Ta base high temperature SMAs. High temperature shape memory effect (*Ms*=460K and *Af* = 490K) was confirmed for a Ti-32Ta alloy during thermal cycling between 173K and 530K under a constant stress. The effect of ternary alloying on the shape memory effect was investigated in order to improve the stability of the shape memory properties against aging effects, and results showed that Al and Sn were effective alloying elements.

Keywords: *shape memory effect, β titanium (Ti)-base alloys, ω-phase, high temperature shape memory alloy*

1. Introduction

Shape memory alloys (SMAs) exhibit unique properties which are the shape memory effect (SME) and superelasticity (SE), so they are promising candidates for applications as actuators and superelastic materials. The applicability of SMA is limited by its martensitic transformation temperatures. Commercially available Ti-Ni SMA is successfully used for many practical applications, but it has martensitic transformation start temperature (*Ms*) below 373K, therefore setting the limitations of its applications. Recently, there has been a growing interest of SMA for applications in automobile engine, aircraft and gas-oil industries, where the operating temperature is above 373K. The addition of ternary elements, such as Zr, Hf, Pd, Au and Pt to Ti-Ni has been reported to be effective to increase the *Ms* above 373K[1-3]. However, all of them exhibit poor cold-workability, therefore they are difficult to fabricate into wires and sheets, for practical applications.

Recently β-type Ti-Nb[4-9], Ti-Mo[10-13] and Ti-Ta[14-15] base alloys, which exhibit excellent cold-workability (thickness reduction>90%), have been reported to exhibit shape memory effect and superelasticity. The shape memory effect in these alloy systems is due to the reversible martensitic transformation between the β-parent phase and the α"-martensite phase. However, Ti-Nb and Ti-Mo base alloys are very sensitive to aging effects at temperatures between 473K and 673K due to the formation of the ω-phase[16], which suppress the martensitic transformation temperatures and cause embrittlement.

It has been reported that addition of Ta to Ti-Nb was effective to suppress the ω-phase formation[5]. Therefore in this study, the development of Ti-Ta base shape memory alloys for high temperature applications is proposed.

2. Experimental Procedure

Ti-32at.%Ta, Ti-22at.%Nb, Ti-30at.%Ta-lat.%Al and Ti-30at.%Ta-1at.%Sn alloys were fabricated by an arc melting method in Ar atmosphere. From here onwards the at.% in composition is omitted. The as-melted ingots were homogenized at 1273K for 7.2ks and then cold rolled up to 98% in thickness reduction, the specimen thickness after cold-rolling was about 100 μm. The specimens for tensile tests and X-ray diffraction (XRD) analysis were cut by an electro-discharge spark-erosion cutting machine. The surface oxides formed during cutting were removed by chemical etching using a solution of 10%HF, 40%HNO_3 and 50%H_2O by volume. Then the specimens were vacuum sealed in a quartz tube filled with high purity Ar gas. The specimens were solution-treated at 1173K for 1.8 ks, followed by water-quenching by breaking the quartz tube in a water bath. After solution-treatment, some of the specimens were aged at various temperatures from 473K to 873K for 3.6ks, followed by water-quenching (WQ). The oxidized surface formed during quenching was removed by chemical etching. The shape memory behavior was characterized by tensile tests under various constant stresses during thermal cycling. The phase constitutions at room temperature were investigated by X-ray diffraction (XRD) analysis using a Cu-Kα X-ray source.

3. Results and discussion

3.1 Shape memory behavior of Ti-22Nb and Ti-32Ta

Figure 1(a) shows the strain-temperature curves of Ti-32Ta solution-treated (ST) alloy. The strain-temperature curves were obtained from the tensile test under various constant stresses during thermal cycling. Initially a tensile load of 25MPa was applied, and then the specimen was heated up to 530K at 10K/min. A shape recovery is observed at about 490K due to the reverse martensitic transformation. Then the applied load was increased to 50MPa and thermal cycling was performed, and after each thermal cycle the load was increased to a higher stress. The cooling and heating cycles are represented as solid and dashed lines, respectively. The martensitic transformation start and reverse martensitic transformation finish temperatures are indicated as, *Ms* and *Af*, respectively. On cooling, tensile elongation (shape deformation) was observed, which is due to the martensitic transformation. On heating, the elongated specimen undergoes shape recovery due to the reverse martensitic transformation. Although the *Ms* and *Af* decreased during thermal cycling they remained above 373K.

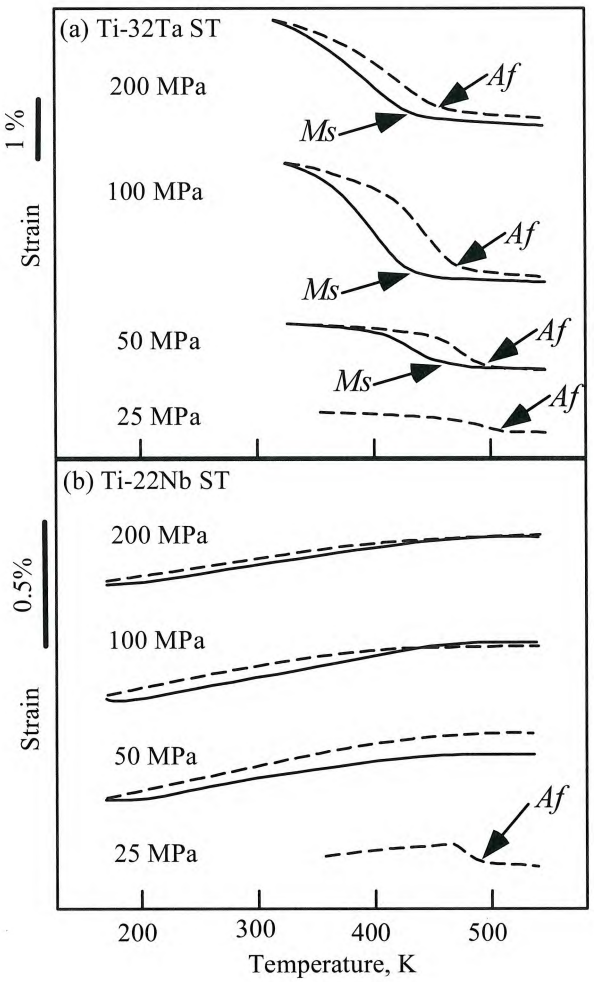

Figure 1. Strain-temperature curves of a) Ti-32Ta and b) Ti-22Nb solution-treated (ST) alloys. The solid lines correspond to the cooling cycle and the dashed lines correspond to the heating cycle.

The strain-temperature curve of a Ti-22Nb ST specimen obtained by a similar experiment is shown in Figure 1(b). The specimen during the first heating under a 25MPa load revealed the reverse martensitic transformation at 490K, indicating the reverse martensitic transformation temperature of Ti-22Nb is similar to that of Ti-32Ta. However, during the succeeding thermal cycles at a constant stress of 50 to 200 MPa, the shape memory effect was not observed in Ti-22Nb alloy.

Figure 2 shows X-ray diffraction (XRD) profiles taken at room temperature for Ti-22Nb (a) ST and (b) ST followed by aging at 573K for 3.6ks. The diffraction peaks of Cu were obtained from a specimen holder. The ST specimen revealed α"-martensite phase, indicating that *Ms* is above room temperature. On the other hand, the specimen aged at 573K for 3.6 ks revealed the presence of β-phase matrix and ω-phase precipitates. The composition of the ω-phase is Ti-rich when compared with the Ti-content of the β-phase matrix, therefore when the ω-phase precipitated during aging then the composition of the matrix changed such that the nominal content of Nb in the matrix increased. It was reported that with increasing Nb content in Ti-Nb alloys the *Ms* decreases by 40K per lat.% Nb[4-9], thus the increase in the nominal content of Nb in the matrix shifted the *Ms* to a lower temperature.

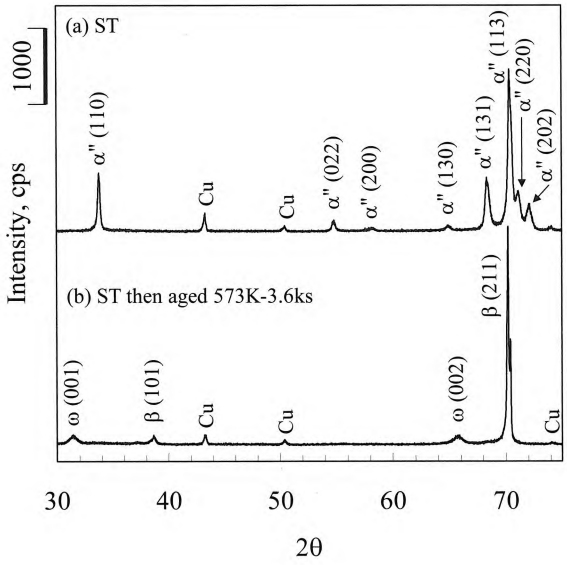

Figure 2. XRD profiles of Ti-22Nb (a) solution-treated (ST) and (b) ST then aged at 573K for 3.6ks.

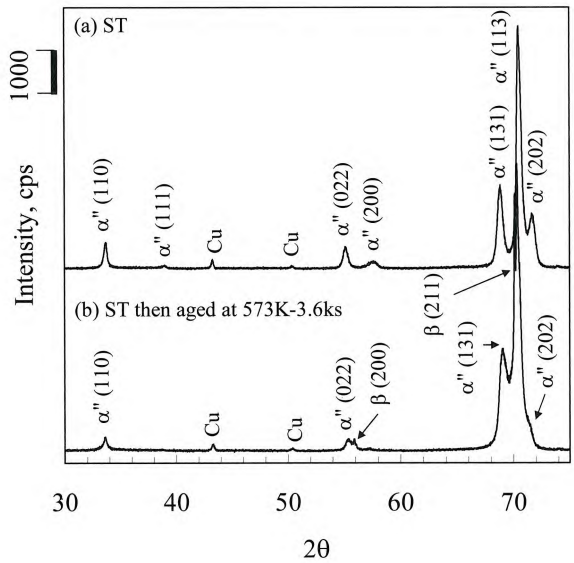

Figure 3. XRD profiles of Ti-32Ta (a) solution-treated (ST) and (b) ST then aged at 573K for 3.6ks.

In addition, the presence of ω-phase precipitates within the matrix (the precipitates was confirmed by TEM, but the photomicrograph is not shown here) is suggested to suppress the martensitic transformation process. This is because they act as an obstacle to the interface between β-phase and α"-martensite phase during martensitic transformation. As a result, it is supposed that the formation of ω-phase during thermal cycling suppressed the shape memory effect of Ti-22Nb alloy, as shown in Figure 1(b).

Figure 3 shows XRD profiles taken at room temperature for Ti-32Ta (a) ST and (b) ST followed by aging at 573K for 3.6ks. The *Ms* for the ST alloy is about 460K, thus it is reasonable that the existing phase at room temperature is α"-martensite phase as revealed in the XRD profile. Whereas the specimen aged at 573K for 3.6ks revealed the presence of α"-martensite phase and β-phase. The presence of α"-martensite phase indicate that the *Ms* remained above room temperature after aging, but the

appearance of β-phase means that the transformation temperature decreased compared to the ST specimen. There was no ω-phase confirmed for this specimen suggesting that Ti-32Ta alloy is less sensitive to aging when compared with Ti-22Nb alloy. As a result shape memory effect was observed for Ti-32Ta ST alloy during repeated thermal cycling up to 530K as shown in Figure 1(a).

3.2 Aging temperature dependence of *Ms* and *Af* of Ti-32 Ta alloy

Figure 4 shows the plot of *Ms* and *Af* of Ti-32Ta alloy which were solution-treated followed by aging at different temperatures for 3.6ks. The transformation temperatures were measured from the strain-temperature curve at a constant stress of 50MPa. The *Ms* and *Af* of the alloys revealed a strong dependence on the aging temperature. With increasing aging temperature from 473 to 573K the *Ms* and *Af* decreased, and then from 573 to 873K they increased until they reached a similar transformation temperatures as with the ST specimen. Although there was no ω-phase from the XRD profile of the aged specimen (figure 3(b)), the appearance of diffraction peaks corresponding to the β-phase after aging means that the *Ms* of the matrix decreased. This is probably due to the formation of very fine ω-phase, which can not be detected by XRD. The significant decrease in the transformation temperature by aging at 573K for 3.6ks means that the aging effect in the binary Ti-32Ta alloy cannot be suppressed completely. The effect of ternary alloying element was investigated in order to improve the stability of the shape memory properties against aging.

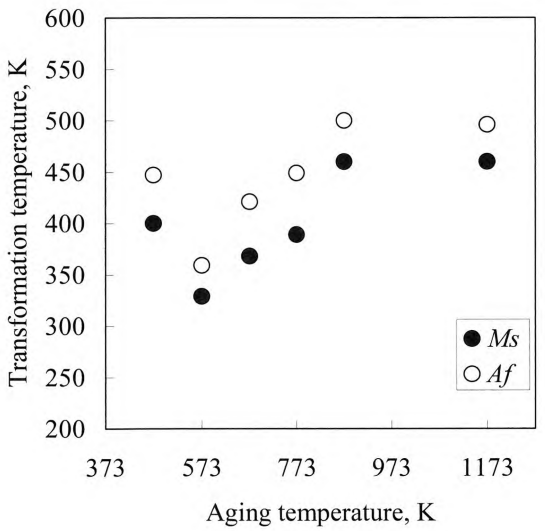

Figure 4. Effect of aging temperature on the *Ms* and *Af* of solution-treated Ti-32Ta. The aging time was constant at 3.6ks.

3.3 Effect of ternary alloying element on the shape memory behavior of Ti-Ta-X alloys

Several ternary alloying elements were investigated in order to identify which elements are effective in improving the stability of the shape memory behavior in Ti-Ta base alloy against the effect of aging at 573K. Figure 5 shows the (a) *Ms* and (b) *Af* of ST and aged (573K for 3.5ks) Ti-32Ta, Ti-30Ta-1Al and Ti-30Ta-lSn alloys, respectively. The transformation temperatures were obtained from the strain-temperature curve for each alloy. For Ti-32Ta, both *Ms* and *Af* significantly decreased by aging at 573K for 3.6ks, whereas the decrease by aging were significantly less for Ti-30Ta-1A1 and Ti-30Ta-1Sn alloys. Therefore, it is suggested that Ti-Ta-Al and Ti-Ta-Sn alloys are promising candidate materials as high temperature shape memory alloy. Further investigation is needed to determine the appropriate composition of the ternary alloy systems that exhibit *Ms* above 373K and stable shape memory behavior against aging effects.

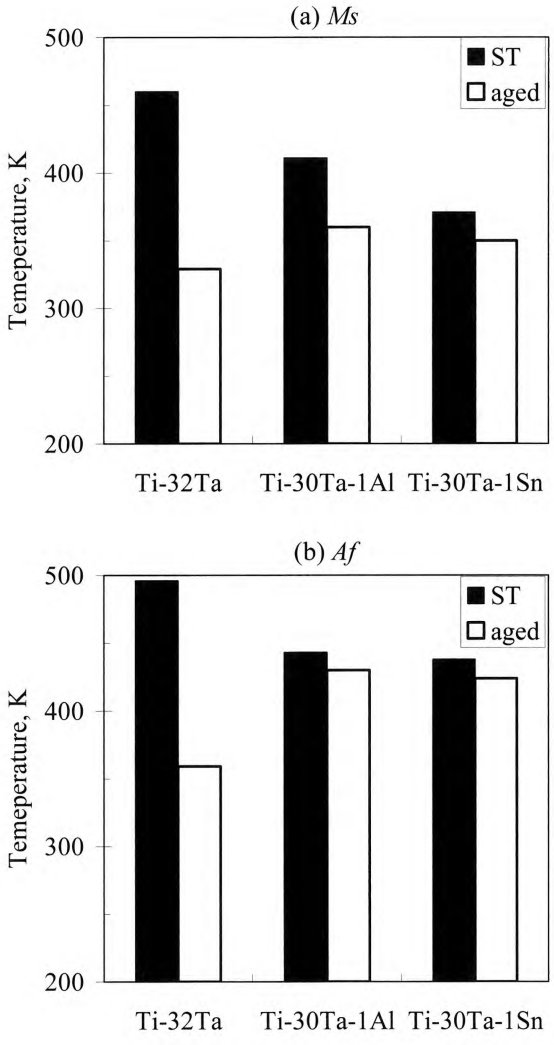

Figure 5. (a) *Ms* and (b) *Af* of solution-treated (ST) and aged (573K for 3.6ks) Ti-32Ta, Ti-30Ta-1Al and Ti-30Ta-1Sn alloys, respectively.

4. Conclusions

High temperature shape memory effect was confirmed for Ti-32Ta alloy, where *Ms*=460K and *Af*=490K. However, by aging at 573K for 3.6ks the *Ms* and *Af* significantly decreased. The decrease in transformation temperature due to aging at 573K was successfully suppressed by the addition of Al and Sn as ternary alloying elements.

Acknowledgement
This work was partially supported by ILC Project from University of Tsukuba, the 21 Century Center of Excellence Program, the Iketani Foundation and the Grants-in-Aid for Fundamental Scientific Research (Wakate B(2006-2007)) from the Ministry of Education, Culture, Sports, Science and Technology, Japan.

REFERENCES
1) G.S. Firstov, J.Van Humbeeck and Y.N. Koval: Mater. Sci. Eng. A **378** (2004) pp. 2-10.
2) G.S. Firstov, J.Van Humbeeck and Y.N. Koval, Scripta Mater. **30** (2004) pp. 243-248.
3) H.C. Donkersloot and J.H.N. Van Vucht: J.Less-Common Metals **20** (1970) pp. 83-91.
4) S. Miyazaki, H.Y. Kim and H. Hosoda: Mater. Sci. Eng. A **438** (2006) pp. 18-24.
5) H.Y. Kim, S. Hashimoto, J.I. Kim, T. Inamura, H. Hosoda and S. Miyazaki: Mater. Sci. Eng. A **417** (2006) pp. 120-128.
6) H.Y. Kim, Y. Ikehara, J.I. Kim, H. Hosoda and S. Miyazaki: Acta Mater. **54** (2006) pp. 2419-2429.
7) H. Matsumoto, S. Watanabe and S. Hanada: Mater. Trans. **46-5** (2005) pp. 1070-1078.
8) T. Inamura, Y. Fukui, H. Hosoda, K. Wakashima and S. Miyazaki: Mater. Sci. Eng. C **25-3** (2005) pp. 426-432.
9) H.Y. Kim, Y. Ohmatsu, J.I. Kim, H. Hosoda and S. Miyazaki: Mater. Trans. **45** (2004) pp. 1090-1095.
10) H.Y. Kim, Y. Ohmatsu, J.I. Kim, H. Hosoda and S. Miyazaki: Mater. Trans. **47** (2006) pp. 518-522.
11) T. Maeshima, S.Ushimaru, K. Yamauchi and M. Nishida: Mater. Sci. Eng. A **438** (2006) pp. 844-847.
12) T. Maeshima and M. Nishida: Mater. Trans. **45** (2004) pp. 1096-1100.
13) T. Maeshima and M. Nishida: Mater. Trans. **45** (2004) pp. 1101-1105.
14) M. Ikeda, S.Y. Komatsu and Y. Nakamura: Mater. Trans. **45** (2004) pp. 1106-1112.
15) M. Ikeda, Y. Nakamura, and N. Takahama: J. Japan Inst. Metals **67** (2003) pp. 420-423.
16) B.S. Hickman: J. Mater. Sci. **4** (1969) pp. 554-563.